3D localized lactate detection in muscle tissue using double quantum filtered ^{1}H MRS with adiabatic refocusing pulses at 7 T

October 8, 2021

Fabian Niess[1,2], Sigrun Roat[2], Wolfgang Bogner[3], Martin Kršňák[1] Graham J. Kemp[4], Albrecht I. Schmid[2], Siegfried Trattnig[3], Ewald Moser[2], Maxim Zaitsev[2], Martin Meyerspeer[2]

[1]Department of Medicine III, Division of Endocrinology and Metabolism, Medical University of Vienna, Austria [2]High Field MR Center, Center for Medical Physics and Biomedical Engineering, Medical University of Vienna, Austria [3]High Field MR Center, Department of Biomedical Imaging and Image-guided Therapy, Medical University of Vienna, Austria [4]Department of Musculoskeletal and Ageing Science, Institute of Life Course and Medical Sciences, University of Liverpool, Liverpool, UK.

Correspondence to:
Assoc. Prof. Dipl.-Ing. Dr. techn. Martin Meyerspeer
Center of Medical Physics and Biomedical Engineering
High Field MR Center
Medical University of Vienna
A-1090 Wien, Lazarettgasse 14
Austria
Tel: +43 1 40400 64610
Email: martin.meyerspeer@meduniwien.ac.at

Running title: 3D-localized double quantum filtered lactate detection in muscle at 7 T
Word Count: 3200
Abstract Word Count: 198
Keywords: skeletal muscle exercise, localized 1H-MRS, double quantum filter, ultra-high field, lactate

Abstract

Purpose

Lactate is a key metabolite in skeletal muscle and whole-body physiology. Its MR visibility in muscle is affected by overlapping lipid signals and fiber orientation. Double quantum filtered (DQF) 1H-MRS selectively detects lactate at 1.3 ppm, but at ultra-high field the efficiency of slice-selective 3D-localization with conventional RF pulses is limited by bandwidth. This novel 3D-localized 1H-DQF-MRS sequence uses adiabatic refocusing pulses to unambiguously detect lactate in skeletal muscle at 7 T.

Methods

Lactate double quantum coherences were 3D-localized using slice-selective Shinnar-Le-Roux optimized excitation and adiabatic refocusing pulses (similar to semi-LASER). DQF MR spectra were acquired at 7 T from lactate phantoms, meat specimens with injected lactate (exploring multiple TEs and fiber orientations) and human gastrocnemius in vivo during and after exercise (without cuff ischemia).

Results

Lactate was readily detected, achieving the full potential of 50 % signal with a DQF, in solution. The effects of fiber orientation and TE on the lactate doublet (peak splitting, amplitude and phase) were in good agreement with theory and literature. Exercise-induced lactate accumulation was detected with 30 s time resolution.

Conclusion

This novel 3D-localized 1H-DQF-MRS sequence can dynamically detect glycolytically-generated lactate in muscle during exercise and recovery at 7 T.

Keywords: skeletal muscle exercise, localized 1H-MRS, double quantum filter, ultra-high field, lactate

1 Introduction

Lactate is an important biomarker of energy metabolism. In clinical studies elevated lactate levels are linked to disease outcomes in, e.g., critical illness [1], cancer [2] and mitochondrial dysfunction [3, 4], and failure of lactate accumulation in exercising muscle can indicate glycolytic defects [5]. Once considered a waste product of glycolysis, lactate is today recognized as a key metabolite for skeletal muscle and whole-body physiology, circulating as a major carbohydrate fuel [6–8], and shuttling intra- and inter-cellularly as a gluconeogenic and oxidative substrate [9–11]. Lactate is produced by reduction of glycolytically-generated pyruvate [12,13] in the anaerobic synthesis of adenosine triphosphate (ATP) by substrate-level phosphorylation; ATP is also produced by substrate-level phosphorylation at the expense of phosphocreatine and by oxidative phosphorylation in the aerobic metabolism mainly of carbohydrates and lipid. These three processes maintain homeostasis in the face of potentially high ATP demands of muscle force production [14, 15]; their relative contributions are regulated depending on the intensity and duration of exercise [15], in ways that are still not fully understood (see e.g., [13]). For a better understanding of this interplay, dynamic monitoring of energy metabolites is required, ideally by non-invasive means.

Magnetic resonance spectroscopy (MRS) offers many non-invasive quantitative insights into muscle energy metabolism [13, 16–20]. Lactate can be accessed directly using ^{1}H-MRS, but its quantification in skeletal muscle is challenging. Firstly, large lipid signals overlap the main lactate resonance, the methyl group doublet at 1.3 ppm. Even at long echo times (T_E) residual lipid signals dominate at $0.9 - 1.5$ ppm. Spectral subtraction of averaged pre- and post-exercise ^{1}H-MR spectra, acquired from the forearm muscle using STEAM ($T_\mathrm{E} = 140$ ms), has been used to eliminate residual lipid signals [21]. However, this introduces strong motion-sensitivity, which may lead to imperfect lipid nulling and consequently inaccurate absolute lactate quantification: this is particularly challenging in dynamic exercise experiments. A second problem is that orientation-dependent dipolar coupling effects significantly alter the apparent scalar modulation constant of the lactate methyl group in muscle tissue. Dipolar splitting obeys the orientation dependence of magnetic dipole-dipole interaction and is caused by incomplete motional averaging [22, 23]. According to a model developed using the product operator formalism, the lactate methyl signal acquired with a double quantum filtered (DQF)

pulse sequence [24] attains its maximum for muscle fibers orientated parallel to the main magnetic field B_0 and setting the effective echo time to 30 ms, with asymmetric composition of T_E, i.e. $(\tau_1, \tau_2) = (10\,\text{ms}, 20\,\text{ms})$. Increasing the angle between muscle fibers and B_0 decreases the detectable lactate signal, while additionally increasing the respective optimum T_E (e.g. 37 ms for 24° and 57 ms for 33°) [25]. Inappropriate combinations of fiber orientation and sequence timing can even lead to complete loss of lactate visibility [24, 26, 27].

DQF ^{1}H-MRS offers a single-shot approach to selectively acquire the lactate resonance at 1.3 ppm, while entirely removing overlapping lipid resonances [28, 29]. Recently published experts consensus papers on ^{1}H-MRS have mentioned DQF spectroscopy as the preferred method for unambiguous lactate quantification [20, 30]. Several spatial localization schemes have been combined with DQF spectroscopy for lactate detection, including stimulated-echo-acquisition-mode (STEAM) [31], chemical-shift-imaging (CSI) [29] and point-resolved spectroscopy (PRESS) [25, 32, 33]. However, ^{1}H-DQF-MRS inherently sacrifices 50 % of the achievable signal-to-noise ratio (SNR) [34]. Given the relatively low lactate concentrations produced during sub-maximal exercise (e.g., 7 mmol kg^{-1} [35]), in vivo quantification using MRS remains challenging, especially when localizing to a specific muscle group. Exercise under cuff ischemia can achieve much higher muscle lactate levels (inhibiting both vascular oxygen supply and lactate clearance), as seen in our study using 3D-localized ^{1}H-DQF-MRS at 3 T [25]. But this is often not feasible or well-tolerated, particularly by subjects in clinical research, and limits studying the physiology across the range of normal activity.

Applying localized ^{1}H-DQF-MRS at 7 T, with significantly increased SNR compared to 3 T, allowed Boer et al. [36] to detect lactate in human calf muscle using slice-selective excitation followed by frequency-selective pulses for double quantum editing. However, this came at the cost of losing 3D-localization, and signal was acquired from the entire transversal slab [36]. The ability to accurately localize a 3D volume of interest on ultra-high field (UHF) whole-body systems is limited by the bandwidth achievable with classical RF-pulses. Additionally, low refocusing pulse bandwidth, and hence high chemical shift displacement, interferes with the coherence transfer pathways in DQF sequences and leads to a reduced detection sensitivity of lactate [33]. Adiabatic RF-pulses allowed for a higher bandwidth, are insensitive to B_1^+ inhomogeneities [37] and are extensively used for slice-selective refocusing in established single-voxel spectroscopy sequences such as semi-LASER [38].

Here, we present a novel acquisition scheme to acquire 3D-localized selective ^{1}H-DQF-MR spectra with adiabatic slice-selective refocusing for unambiguous lactate detection in skeletal muscle tissue at UHF of 7 T.

2 Methods

2.1 MR Pulse Sequence

Following a WET [39] water suppression scheme the localization of the lactate signal to a user-defined 3D volume was performed similarly to semi-LASER using perpendicular slice-selective excitation and adiabatic refocusing [38, 40]. A Shinnar-Le-Roux optimized excitation pulse (pulse duration: 2.6 ms, bandwidth: 3.3 kHz) and two pairs of adiabatic full passage pulses (AFP smoothed chirp, duration: 4.6 ms, bandwidth: 5 kHz) were used. Time delays between pulses were adjusted individually, to achieve either symmetric ($\tau_1 = \tau_2$) or asymmetric ($\tau_1 \neq \tau_2$) composition of the overall echo time, ($T_\mathrm{E} = \tau_1 + \tau_2$), see Figure 1.

[Figure 1 about here.]

To detect the methyl group of lactate at 1.3 ppm while removing overlapping extra- and intracellular lipid resonances, double quantum coherences (DQC) of the scalar coupled spin system were created and selected using additional 90° pulses and de- and rephasing gradients (moment ratio 1:2) see Figure 1. After a delay of 1/2J a non-selective rectangular pulse converts the single quantum coherences (SQC) into invisible double and zero quantum coherences, which are affected differently by the subsequent dephasing gradient (DQCs are twice as sensitive to gradients compared to SQCs, while ZQCs are unaffected). Then a frequency-selective 90° pulse on the methine group of lactate (at 4.11 ppm, phantom: RF bandwidth 120 Hz, in vivo: RF bandwidth 200 Hz) reverts the magnetization back into an observable single quantum state, and during 1/2J the magnetization is refocused. Only the magnetization components that evolved as DQC between the two 90° pulses are rephased by the rephasing gradient shortly before readout, while other contributions are dephased due to these unbalanced gradients. To minimize chemical shift displacement artifacts a frequency offset relative to the water resonance was added to the localization pulses to target the methyl group of lactate at 1.3 ppm.

2.2 Phantom and ex vivo Measurements

First, the sequence was tested using a spherical phantom (160 mm diameter) filled with lithium lactate (96 mM) and sodium acetate (100 mM). Spectra were acquired from a 27 ml volume with $T_R = 3\,s$ and $T_E = 135\,ms$. The DQF-sLASER sequence was compared to DQF-PRESS using a spherical phantom (100 mm diameter) filled with aqueous sodium lactate (60 % weight per weight). Spectra from a 16 ml volume were acquired with identical parameters ($T_R = 3\,s$, $T_E = 135\,ms$, refocusing pulse duration: 6 ms). Additionally, the influence of varying the interval τ_m in the DQF-sLASER sequence was investigated. Next, to investigate fiber orientation-dependence, a porcine meat specimen injected with 30 ml aqueous sodium lactate (60 % w/w) was measured repeatedly, orienting it (plus coil) at 4 angles from 0° to 45° relative to B_0. T_E was modulated between 56 and 200 ms with symmetric ($\tau_1 = \tau_2$) and asymmetric composition (holding either τ_1 or τ_2 at minimum).

Spectra were acquired from a 17 ml volume with $T_R = 3\,s$. De- and rephasing gradient moments to select DQCs were set to $16\,ms \cdot mT/m$ and $32\,ms \cdot mT/m$, respectively (amplitude: 20 mT/m, duration: 0.8 ms/1.6 ms). Experiments were conducted within 3 to 16 days after lactate injection, the specimen was stored at 8 °C and brought to room temperature before measurements.

2.3 In vivo Measurements

Five healthy subjects (2 f / 3 m, BMI: $21 \pm 1\,kg/m^2$, age: $33 \pm 4\,y$) participated, providing full written informed consent to the protocol approved by the local research ethics committee. Using 25 transversal imaging slices of the calf, which were acquired with a multi-slice gradient-echo sequence, the voxel (84 ± 13 ml) was carefully positioned in the gastrocnemius muscle close to the coil, covering both g. lateralis and g. medialis. Following semi-LASER ^{1}H-MRS reference scans with and without water suppression, subjects underwent an exercise-recovery protocol to induce lactate production. The protocol consisted of 2 min rest, 3 min straight-knee plantar flexion exercise and 12 min recovery. No cuff ischemia was used. Data were continuously acquired throughout the experiment using the DQF-sLASER acquisition scheme described above. The subjects were instructed to perform a single pedal push between each acquisition ($T_R = 3\,s$), using a custom-built non-magnetic pneumatic ergometer

(similar to [41]), inflated manually with air to achieve an exercise intensity of 45 % of each subject's maximum voluntary contraction force (MVC), which had been measured on the same ergometer.

To suppress the lipid signal in vivo, dephasing and rephasing gradient moments were set to 277 ms · mT/m and 554 ms · mT/m (ratio 1:2) respectively (amplitude: 49.5 mT/m, duration: 5.6 ms/11.2 ms), in accordance with [36]. To achieve 49.5 mT/m two orthogonal gradients with 35 mT/m amplitude were played out simultaneously, see Figure 1. The interval τ_{m} was set to 9 ms and the overall echo time T_{E} to 84 ms ($T_{\mathrm{E}} = \tau_1 + \tau_2 = 42 + 42$ ms). Dephasing of the lipid resonances was confirmed by acquiring an additional reference scan (10 averages) prior to the exercise-recovery protocol using the DQF-sLASER acquisition scheme and setting the voltage for the frequency-selective 90 ° pulse (Gaussian at 4.11 ppm) to 0 V. Following exercise-recovery, additional semi-LASER ^{1}H reference scans were acquired with and without water suppression to account for potential frequency drifts.

2.4 Experimental Setup

All measurements were conducted on a Siemens Terra dot Plus 7T scanner (Siemens, Erlangen, Germany). For phantom measurements a surface coil with a single transmit/receive ^{1}H loop ($\sim$ 10 cm, RAPID Biomedical GmbH, Germany) was used, while measurements on meat specimens and in vivo were performed with a custom-built surface coil array with two transmit/receive ^{1}H loops, form-fitted to the anatomy of the human calf [42]. The coils' available ^{31}P elements were not used.

2.5 Postprocessing

^{1}H-MR spectra were extracted and processed from the Siemens raw data format using in-house Python scripts (http://www.python.org) including phasing and channel combination. Phasing was performed to the highest peak amplitude of post exercise lactate at 1.3 ppm for each channel before summation. The lactate doublet at 1.3 ppm was quantified using jMRUI [43] with the fitting routine AMARES [44]. Sensor data from the ergometer were acquired using the Labjack U6 multifunction device (https://labjack.com) and in-house Python scripts.

3 Results

In solution (Figure 2a) the lactate doublet at 1.3 ppm (peak splitting $J = 7.3$ Hz) was successfully quantified using the novel DQF-sLASER acquisition scheme. Compared to conventional semi-LASER, DQF spectra achieved 53 % and 49 % of the integrated signal area in a repeated experiment. In addition to that, increasing τ_{m} to 9 ms caused a minor signal reduction of 4 % compared to the minimum achievable of 3 ms. In contrast, DQF-PRESS achieved only 3.5 % of the integrated signal area compared to regular PRESS. Resonances such as sodium acetate (~ 1.9 ppm, spherical phantom) or lipid signals ($0.9 - 1.5$ ppm, ex vivo and in vivo) were suppressed almost entirely by the unbalanced gradients (1:2) with DQF-sLASER.

In the meat specimen, the injected sodium lactate gave rise to a doublet (Figure 2b), with an increased peak splitting compared to lactate in solution, due to orientation-dependent effects (dipolar coupling (Δ_{dc}), such that $\Delta = \Delta_{\mathrm{dc}} + J = 13$ Hz [24]). The fiber orientation is a vector in 3D, and its angle α relative to the z-direction is therefore defined by

[Figure 2 about here.]

a component φ in the coronal plane (visible as striation in Figure 3b) and the inclination ϑ in the sagittal plane (Figure 3c). A rotation of the coil on the patient table by Φ (together with the meat specimen) only affects the coronal component, and the effective fiber angle α relative to $\vec{B}_0$ can be calculated via $\tan^2\alpha = \tan^2(\Phi - \varphi) + \tan^2\vartheta$. This resulted in $\alpha \approx 41°$ for $\Phi = 0°$ and $\alpha \approx 16°$ for $\Phi = 45°$.

[Figure 3 about here.]

This affected the splitting of the lactate doublet, varying from 13 to 20 Hz (Figure 4). Signal modulations of the lactate doublet were observed with increasing T_{E}, showing signal nulling and negative amplitudes for echo times with either τ_1 or τ_2 held constant. Fiber angles with a more parallel alignment to B_0 showed signal inversion at short T_{E}, in good agreement with simulations [25] and measurements [24, 26]. A separate experiment confirmed that rotating the coil by up to 45° relative to B_0 caused a minor effective reduction of B_1^+ below 10 %, due to the resulting suboptimal transmit phase offset per channel and varying B_1 component in z-direction.

[Figure 4 about here.]

In vivo (Figure 2c), lactate produced during plantar flexion was successfully detected post exercise in gastrocnemius ($\Delta = 22\,\mathrm{Hz}$). Figure 5a shows a representative voxel placement during in vivo measurements on a transversal gradient-echo image of the human calf muscle, covering m. gastrocnemius (medialis and lateralis). Elevated post-exercise lactate was seen in all subjects as a clearly resolved doublet at 1.3 ppm with splitting ranging from 14 to 22 Hz, which corresponds to fibre angles in the range of 11° to 34° [22, 26]. After peaking $\sim 1\,\mathrm{min}$ post-exercise, the lactate signal decreased continuously towards noise level throughout the recovery. At rest and during exercise, no lactate resonance could be detected above noise level. Figure 5b shows the time-course of fitted lactate concentrations (corresponding to the sum of integrated areas of the doublet, averaged over all subjects) and representative spectra (average over 10 spectra, i.e., 30 s, per subject) from rest, exercise and recovery.

Averaged frequency drifts calculated over all subjects from pre- and post exercise ^{1}H-semi-LASER reference scans were $5 \pm 3\,\mathrm{Hz}$, which is negligible compared to peak linewidth and splitting.

[Figure 5 about here.]

4 Discussion

This study presents a novel 3D-localized single-shot acquisition scheme to dynamically detect glycolytically-generated lactate using double quantum editing in exercising human muscle tissue at UHF of 7 T. The methyl group of lactate resonating as a doublet at 1.3 ppm was successfully detected in all experiments, all overlapping resonances being suppressed. In phantoms, the DQF-sLASER sequence reached full theoretical efficacy, detecting 50 % of the excitable magnetization.

Pulse durations were chosen to achieve the required 90° flip angles and fulfil the adiabatic condition for full refocusing at the voxel (up to 3 cm distance from the coil), while complying with the hardware constraints and SAR limits. Using DQF spectroscopy together with slice-selective 3D localization at 7 T, the chemical shift displacement needs to be minimized as it interferes with coherence transfer pathways, which significantly affects spatial localization

accuracy and detection sensitivity of lactate [33]. This was confirmed by results acquired using the DQF-PRESS sequence, which showed to be highly inefficient at 7 T. By implementing adiabatic full passage pulses for slice-selective refocusing, the time-bandwidth-product increased by almost 4-fold compared to conventional MAO pulses used e.g. in PRESS (22.8 ms·kHz vs. 6 ms·kHz), hence, significantly reducing chemical shift displacement with DQF-sLASER.

Results from the porcine meat using different orientations of the coil relative to B_0 are shown in Figure 4. Both the increased splitting of the lactate doublet upon closer alignment of muscle fibers to B_0 and the observed signal evolution for an asymmetric composition of the overall T_E are in good agreement with simulations and literature results [24, 25]. Especially the correlation between the peak splitting of the lactate doublet and the measured fiber orientation is in excellent agreement with literature [26], see Figure 4e. In theory, an asymmetric composition offers maximum lactate signal for a specific fiber angle, but is more sensitive to subtle changes in orientation compared to a symmetric composition [25]. This is in good agreement with results presented in Figure 4. The coil orientation with a maximum angle of 45° had a minimal effect on B_1^+ with a reduction of $< 10\,\%$ compared to 0°, negligible in context, since the goal was to measure the signal modulation with T_E for different angles and not to compare signal intensities between different coil orientations. The signal intensity simulated in [25] comprises contributions from intra- and extracellular components with different T_2s and Δs. The intra- vs. extracellular fraction are certainly different in vivo and in a meat specimen infused with lactate, in which lactate concentrations will presumably equilibrate during the several days after injecting the lactate, and fiber orientation may have been heterogeneous in our selected voxel. The evolution of signal with T_E will therefore be quantitatively different, in vivo. Hence rotating a meat specimen serves as illustration and qualitative proof that fiber orientation does in fact influence the peak splitting of the lactate doublet at 1.3 ppm. The position of zero-crossing (with asymmetric τ combinations) indicate that orientation effects have indeed an effect on echo-time dependence of the DQF signal. The setting of our experiments on meat however comes with the limitations of uncertain fibre orientation (in particular regarding φ), cell membrane integrity, repositioning accuracy between orientations (measured on different days) and uncertain T_2s of the compartments.

For the selection of DQCs in vivo, gradient moments had to be drastically increased to $277\,\mathrm{ms}\cdot\mathrm{mT/m}$ and $554\,\mathrm{ms}\cdot\mathrm{mT/m}$ (ratio 1:2), respectively, compared to $16\,\mathrm{ms}\cdot\mathrm{mT/m}$ and

$32\,\mathrm{ms} \cdot \mathrm{mT/m}$ for phantom and ex vivo measurements. This could be because the temperature of the porcine specimen was lower compared to in vivo measurements and the viscosity of intra/intermuscular fat is higher at lower temperature, leading to shorter T_2. Gradient moments used in vivo were only slightly higher to values proposed by Boer et al. [36], the difference probably being due to our more sensitive coil type (surface coil instead of volume coil). Although the plantar flexions were performed between DQF-sLASER acquisitions to avoid motion, lactate could not be reliably detected during exercise. This might be due to sensitivity to tissue motion on a microscopic (e.g. pulsation) or macroscopic scale (e.g. repositioning of the muscle between pedal pushes).

To confirm that the acquired signal cannot be confused with overlapping lipid signals but indeed reflects the lactate methyl group, we performed a similar reference scan prior to the exercise-recovery experiment as in [36] by setting the pulse voltage for the frequency-selective 90° pulse to 0 V. In contrast to [36] we did not observe lactate signals during rest when compared to scans with the frequency selective RF pulse switched on.

The T_E of 84 ms ($42 + 42$ ms) used in vivo was not optimized to fully account for muscle fiber orientations, but covers a broad range of assumed fiber orientations (in m. gastrocnemius between $\sim$ 24° and 35° [25]) to prove the functionality of the sequence. The measured lactate doublet's splitting corresponds to realistically close to these numbers. A symmetric composition of τ_1 and τ_2 should avoid possible signal nulling, in accordance with simulations [25]. Therefore it is not feasible in this work to achieve a meaningful estimation of lactate concentration, as true compensation of dipolar coupling effects by T_E optimization requires knowledge of muscle fiber orientation, ideally measured prospectively. Also the ratio between lactate concentrations in the intra- and extra-cellular compartments with different T_2 and couplings influences the DQF lactate signal. This ratio is presumably time-dependent, with accumulation starting in intracellular and wash-out via extracellular space, and affected by, e.g., exercise (power, type, duration etc.) and blood perfusion, which should be controlled or quantified [19]. This and estimations of compartmentation will be subject of future studies.

The limitations of using adiabatic pulses for slice-selective refocusing are higher SAR and increased minimal T_E, especially in combination with long gradients necessary to select DQCs in vivo. This could be problematic for fiber orientations parallel to B_0, where the maximum signal amplitude of lactate is expected for T_Es below 40 ms [25]. One way to

address this would be to use global fat inversion prior to excitation and shorter de- and rephasing gradients, at the cost of SNR. The signal models [24, 26] may need to be extended to account for magnetization evolution during the RF pulses, which is likely to shift the optimum towards longer echo times, which is also qualitatively consistent with our results of measurements in meat (Figure 4).

The relatively large voxel size was chosen to cover both gastrocnemius medialis and lateralis as the main contributors to force during plantar flexion exercise. Both muscle groups are predominantly composed of type II muscle fibers [45], leading to stronger glycolytic contribution to ATP synthesis, and more pronounced acidification during anaerobic exercise compared to other muscle groups, which are considered to work in a more oxidative regime, e.g., m. soleus.

To the best of our knowledge, the present study is the first to present 3D-localized ^{1}H-DQF-MR spectra of lactate acquired in human muscle tissue at 7 T. It is worth mentioning that readily detectable lactate accumulation in vivo was induced by exercise without cuff ischemia. Absolute quantification of lactate was not the focus of this work, but the promising results acquired in vivo demonstrate the sensitivity and functionality of the presented acquisition scheme. To correctly quantify absolute lactate concentrations in skeletal muscle using ^{1}H-MRS, the fiber orientation relative to B_0 and compartmentation has to be taken into account [25].

5 Conclusion

We successfully demonstrated a novel acquisition scheme to detect lactate using 3D-localized ^{1}H-DQF-MR spectra with adiabatic refocusing pulses at 7 T. The relationship between the fiber orientation and the lactate signal amplitude underlines the importance of this phenomenon for future quantitative in vivo studies.

References

[1] Kushimoto S, Akaishi S, Sato T, et al. Lactate, a useful marker for disease mortality and severity but an unreliable marker of tissue hypoxia/hypoperfusion in critically ill patients *Acute Medicine and Surgery.* 2016;3:293-297, doi.org/10.1002/ams2.207.

[2] Yaligar J, Thakur S B, Bokacheva L, et al. Lactate MRSI and DCE MRI As Surrogate Markers of Prostate Tumor Aggressiveness *NMR Biomed.* 2012;25:113-122, doi.org/10.1002/nbm.1723.

[3] Hanisch F, Müller T, Muser A, Deschauer M, Zierz S. Lactate increase and oxygen desaturation in mitochondrial disorders–evaluation of two diagnostic screening protocols *Journal of Neurology.* 2006;253:417-423, doi.org/10.1007/s00415-006-0987-0.

[4] Chi CS, Lee HF, Tsai CR, Chen WS, Tung JN, Hung HC. Lactate peak on brain MRS in children with syndromic mitochondrial diseases *Journal of the Chinese Medical Association.* 2011;74:305-309, doi.org/10.1016/j.jcma.2011.05.006.

[5] Löfberg M, Lindholm H, Näveri H, et al. ATP, phosphocreatine and lactate in exercising muscle in mitochondrial disease and McArdle's disease *Neuromuscular Disorders.* 2001;11:370-375, doi.org/10.1016/S0960-8966(00)00205-4.

[6] Gladden L B. Muscle as a consumer of lactate *Medicine and Science in Sports and Exercise.* 2000;32:764-771, doi.org/10.1097/00005768-200004000-00008.

[7] Rabinowitz J D, Enerbäck S. Lactate: the ugly duckling of energy metabolism *Nature Metabolism.* 2020;2:566-571, doi.org/10.1038/s42255-020-0243-4.

[8] Glancy B, Kane D, Kavazis A N, Goodwin M L, Willis W T, Gladden L B. Mitochondrial lactate metabolism: history and implications for exercise and disease *The Journal of Physiology.* 2021;599:863-888, doi.org/10.1113/JP278930.

[9] Leverve X M, Mustafa I. Lactate: A key metabolite in the interceullular metabolic interplay *Critical Care.* 2002;6:284-285, doi.org/10.1186/cc1509.

[10] Brooks G A. Cell-cell and intracellular lactate shuttles *Journal of Physiology.* 2009;587:5591-5600, doi.org/10.1113/jphysiol.2009.178350.

[11] Baltazar F, Afonso J, Costa M, Granja S. Lactate Beyond a Waste Metabolite: Metabolic Affairs and Signaling in Malignancy *Frontiers in Oncology.* 2020;10:231, doi.org/10.3389/fonc.2020.00231.

[12] Moxnes J F, Sandbakk O. The kinetics of lactate production and removal during whole-body exercise *Theoretical Biology and Medical Modelling.* 2012;9, doi.org/10.1186/1742-4682-9-7.

[13] Kemp G J, Ahmad R E, Nicolay K, Prompers J J. Quantification of skeletal muscle mitochondrial function by ^{31}P magnetic resonance spectroscopy techniques: a quantitative review *Acta Physiol (Oxf).* 2015;213:107-144, doi.org/10.1111/apha.12307.

[14] Spriet L L. ATP utilization and provision in fast-twitch skeletal muscle during tetanic contractions *American Journal of Physiology-Endocrinology and Metabolism.* 1989;257:E595-E605, doi.org/10.1152/ajpendo.1989.257.4.E595.

[15] Hargreaves M, Spriet L L. Skeletal muscle energy metabolism during exercise *Nature Metabolism.* 2020;2:817-828, doi.org/10.1038/s42255-020-0251-4.

[16] Hoult D I, Busby S J, Gadian D G, Radda G K, Richards R E, Seeley P J. Observation of tissue metabolites using ^{31}P nuclear magnetic resonance *Nature.* 1974;252:285-287, doi.org/10.1038/252285a0.

[17] Chance B, Im J, Nioka S, Kushmerick M. Skeletal muscle energetics with PNMR: personal views and historic perspectives *NMR Biomed.* 2006;19:904-926, doi.org/10.1002/nbm.1109.

[18] Kemp G J, Meyerspeer M, Moser E. Absolute quantification of phosphorus metabolite concentrations in human muscle in vivo by ^{31}P MRS: a quantitative review *NMR Biomed.* 2007;20:555-565, doi.org/10.1002/nbm.1192.

[19] Meyerspeer M, Boesch C, Camerone D, et al. ^{31}P magnetic resonance spectroscopy in skeletal muscle: Experts' consensus recommendations *NMR in Biomedicine.* 2020:e4246, doi.org/10.1002/nbm.4246.

[20] Kršš̆ák M, Lindebloom L, Schrauwen-Hinderling V, et al. Proton magnetic resonance spectroscopy in skeletal muscle: Experts' consensus recommendations *NMR Biomed.* 2020:e4266, doi.org/10.1002/nbm.4266.

[21] Ren J, Sherry A D, Malloy C R. Noninvasive Monitoring of Lactate Dynamics in Human Forearm Muscle After Exhaustive Exercise by ^{1}H Magnetic Resonance Spectroscopy at 7 Tesla *Magn Reson Med.* 2013;70:610-619, doi.org/10.1002/mrm.24526.

[22] Kreis R, Boesch C. Liquid-crystal-like structures of human muscle demonstrated by in vivo observation of direct dipolar coupling in localized proton magnetic resonance spectroscopy *J Magn Reson B.* 1994;104:189-192.

[23] Vermathen P, Boesch C, Kreis R. Mapping fiber orientation in human muscle by proton MR spectroscopic imaging *Magn Reson Med.* 2003;49:424-432.

[24] Asllani I, Shankland E, Pratum T, Kushmerick M. Double quantum filtered ^{1}H NMR spectroscopy enables quantification of lactate in muscle *J Magn Reson.* 2001;152:195-202, doi.org/10.1006/jmre.2001.2407.

[25] Meyerspeer M, Kemp G J, Mlynárik V, et al. Direct noninvasive quantification of lactate and high energy phosphates simultaneously in exercising human skeletal muscle by localized magnetic resonance spectroscopy *Magn Reson Med.* 2007;57:654-660, doi.org/10.1002/mrm.21188.

[26] Asllani I, Shankland E, Pratum T, Kushmerick M. Anisotropic orientation of lactate in skeletal muscle observed by dipolar coupling in ^{1}H NMR spectroscopy *J Magn Reson.* 1999;139:213-224, doi.org/10.1006/jmre.1999.1774.

[27] Jouvensal L, Carlier P G, Bloch G. Low visibility of lactate in excised rat muscle using double quantum proton spectroscopy *Magn Reson Med.* 1997;38:706-711, doi.org/10.1002/mrm.1910380505.

[28] Graaf A A De, Luyten P R, Hollander J A Den, Heindel W, Bovée W M M J. Lactate imaging of the human brain at 1.5 T using a double-quantum filter *Magn Reson Med.* 1993;30:231-235, doi.org/10.1002/mrm.1910300212.

[29] He Q H, Shungu D C, Vanzijl P C M, Bhujwalla Z M, Glickson J D. Single-Scan in Vivo Lactate Editing with Complete Lipid and Water Suppression by Selective Multiple-Quantum-Coherence Transfer (Sel-MQC) with Application to Tumors *Journal of Magnetic Resonance, Series B.* 1995;106:203-211, doi.org/10.1006/jmrb.1995.1035.

[30] Choi In-Young, Andronesi Ovidiu C., Barker Peter, et al. Spectral editing in ^{1}H magnetic resonance spectroscopy: Experts' consensus recommendations *NMR in Biomedicine.* 2021;34:e4411, doi.org/10.1002/nbm.4411.

[31] Sotak C H, Freeman D M, Hurd R E. The unequivocal determination of in vivo lactic acid using two-dimensional double-quantum coherence-transfer spectroscopy *Journal of Magnetic Resonance.* 1988;78:355-361, doi.org/10.1016/0022-2364(88)90282-X.

[32] Jouvensal L, Carlier P G, Bloch G. Practical implementation of single-voxel double-quantum editing on a whole-body NMR spectrometer: Localized monitoring of lactate in the human leg during and after exercise *Magnetic Resonance in Medicine.* 1996;36:487-490, doi.org/10.1002/mrm.1910360325.

[33] Lei H, Dunn J. The Effects of Slice-Selective Excitation/Refocusing in Localized Spectral Editing with Gradient-Selected Double-Quantum Coherence Transfer *Journal of Magnetic Resonance.* 2001;150:17-25, doi.org/10.1006/jmre.2001.2304.

[34] Jouvensal L, Carlier P G, Bloch G. Evidence for bi-exponential transverse relaxation of lactate in excised rat muscle *Magn Reson Med.* 1999;41:624-626, doi.org/10.1002/(sici)1522-2594(199903)41:3<624::aid-mrm27>3.0.co;2-w.

[35] Tesch P A, Daniels W L, Sharp D S. Lactate accumulation in muscle and blood during submaximal exercise *Acta Physiology.* 1982:441-446, doi.org/10.1002/nbm.4246.

[36] Boer V O, Luijten P R, Klomp D W. Refocused double-quantum editing for lactate detection at 7 T *Magn Reson Med.* 2013;69:1-6, doi.org/10.1002/mrm.24227.

[37] Tannus A, Garwood M. Adiabatic Pulses *NMR in Biomedicine.* 1997;10:423-434, doi.org/10.1002/(sici)1099-1492(199712)10:8<423::aid-nbm488>3.0.co;2-x.

[38] Scheenen T W, Klomp D W, Wijnen J P, Heerschap A. Short echo time ^{1}H-MRSI of the human brain at 3T with minimal chemical shift displacement errors using adiabatic refocusing pulses *Magn Reson Med.* 2008;59:1-6, doi.org/10.1002/mrm.21302.

[39] Ogg R J, Kingsley R B, Taylor J S. WET, a T1- and B1-Insensitive Water-Suppression Method for in Vivo Localized ^{1}H NMR Spectroscopy *Journal of Magnetic Resonance, Series B.* 1994;104:1 - 10, doi.org/10.1006/jmrb.1994.1048.

[40] Meyerspeer M, Scheenen T, Schmid A I, Mandl T, Unger E, Moser E. Semi-LASER-Localized Dynamic ^{31}P Magnetic Resonance Spectroscopy in Exercising Muscle at Ultra-high Magnetic Field *Magn Reson Med.* 2011;65:1207-1215, doi.org/10.1002/mrm.22730.

[41] Meyerspeer M, Kršňák M, Kemp G J, Roden M, Moser E. Dynamic interleaved ^{1}H/^{31}P STEAM MRS at 3 Tesla using a pneumatic force-controlled plantar flexion exercise rig *Magn Reson Mater Phy.* 2005;18:257-262, doi.org/10.1007/s10334-005-0014-y.

[42] Goluch S, Kuehne A, Meyerspeer M, et al. A form-fitted three channel ^{31}P, two channel ^{1}H transceiver coil array for calf muscle studies at 7T *Magn Reson Med.* 2015;73:2376-2389, doi.org/10.1002/mrm.25339.

[43] Naressi A, Couturier C, Devos J M, et al. Java-based graphical user interface for the MRUI quantitation package *Magn Reson Mater Phy.* 2001;12:141-152, doi.org/10.1007/BF02668096.

[44] Vanhamme L, Boogaart A, Huffel S. Improved method for accurate and efficient quantification of MRS data with use of prior knowledge *J Magn Reson.* 1997;129:35-43, doi.org/10.1006/jmre.1997.1244.

[45] Johnson M A, Polgar J, Weightman D, Appleton D. Data on the distribution of fibre types in thirty-six human muscles. An autopsy study. *J Neurol Sci.* 1973;18:111-129, doi.org/10.1016/0022-510x(73)90023-3.

List of Figures

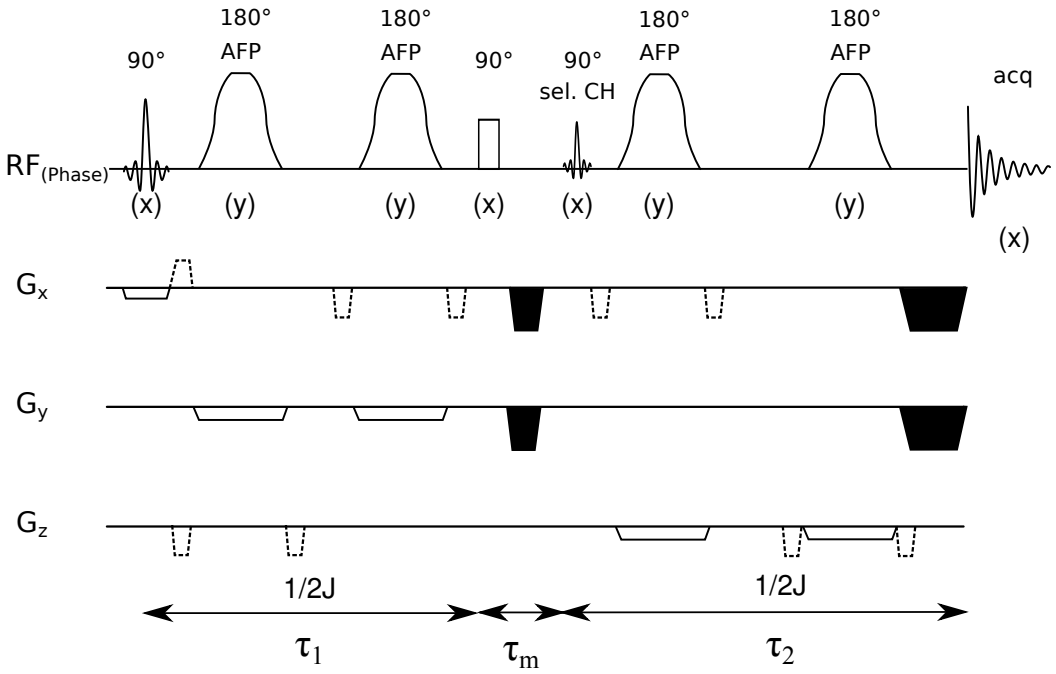

Figure 1: Pulse diagram of double quantum filtered 3D localized ^{1}H MRS using adiabatic slice selective refocusing. During a delay of 1/2J (τ_1) the first four pulses 90°–180°–180°–90° convert the magnetization into a multi-quantum state. The subsequent frequency selective 90° pulse creates anti-phase magnetization, which is refocused during 1/2J (τ_2). DQCs are selected by the de- and rephasing gradients (filled black trapezoids, ratio 1:2) while other non-coupled SQCs are dephased due to unbalanced gradient moments. Slice selection gradients (full trapezoids) and spoiling gradients (dashed trapezoids) are not drawn to scale and intended only to qualitatively illustrate the spoiling scheme.

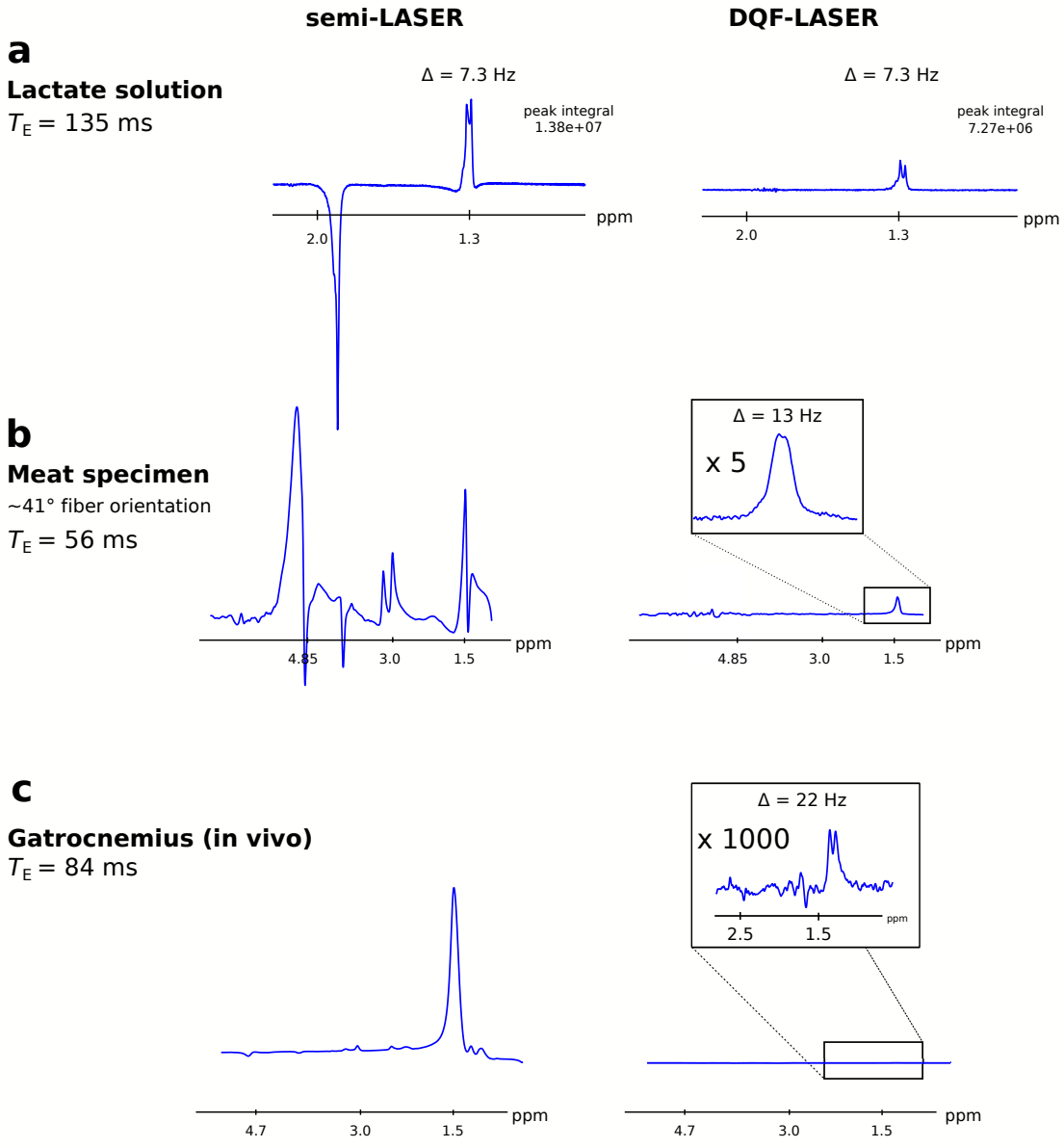

Figure 2: Averaged ^{1}H MR spectra (a/b/c: 10/30/5 averages, $T_R = 3\,s$) acquired using conventional semi-LASER (left) and with the novel DQF-sLASER acquisition scheme (right). Spectra were acquired (a) in vitro from lithium lactate in aqueous solution (96 mM), (b) ex vivo from porcine meat injected with sodium lactate (60 % w/v) and (c) in vivo from m. gastrocnemius of one representative subject. Only lactate is visible in the DQF-sLASER spectra (at 1.3 ppm) with a peak splitting of 7.3/13/22 Hz for a/b/c respectively. Other resonances such as sodium acetate (a), lipid signals and other non-coupled resonances (b, c) were suppressed entirely. The in vivo spectrum showing lactate (c,right) was acquired during the first minute of recovery.

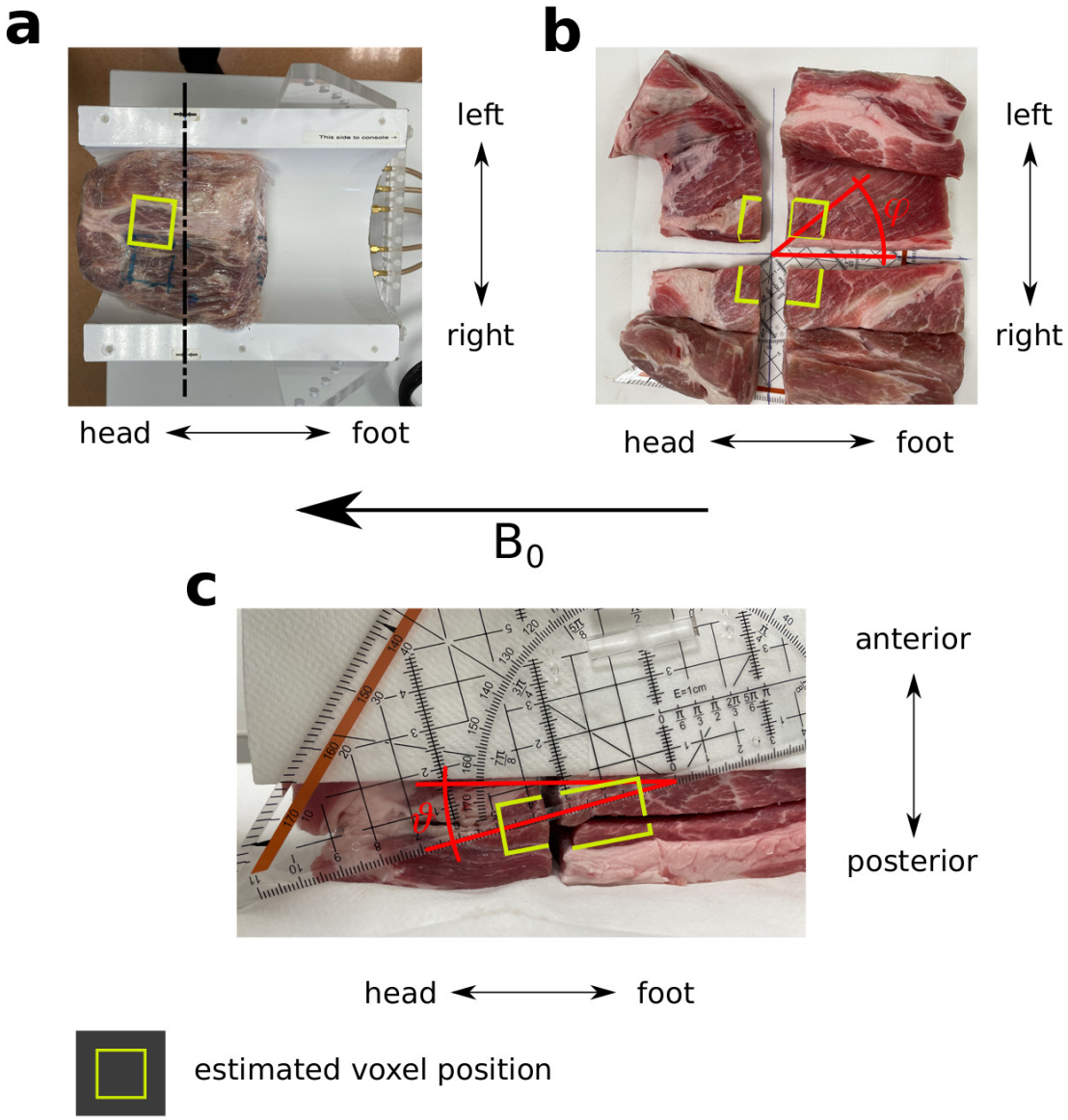

Figure 3: Position of the pork meat specimen placed on the calf coil transceiver array (a). The yellow box illustrates the approximate position of the localized 3D volume of interest where lactate was injected prior to the MR measurement. Estimated fiber angles were $\sim 41°$ ($\varphi \approx 40°$, measured in the coronal plain) for parallel orientation of the coil relative to the B_0 field (b). The inclination in anterior-posterior direction ($\vartheta \approx 15°$) was taken into account for calculating the fiber angle relative to $\vec{B}_0$ (c).

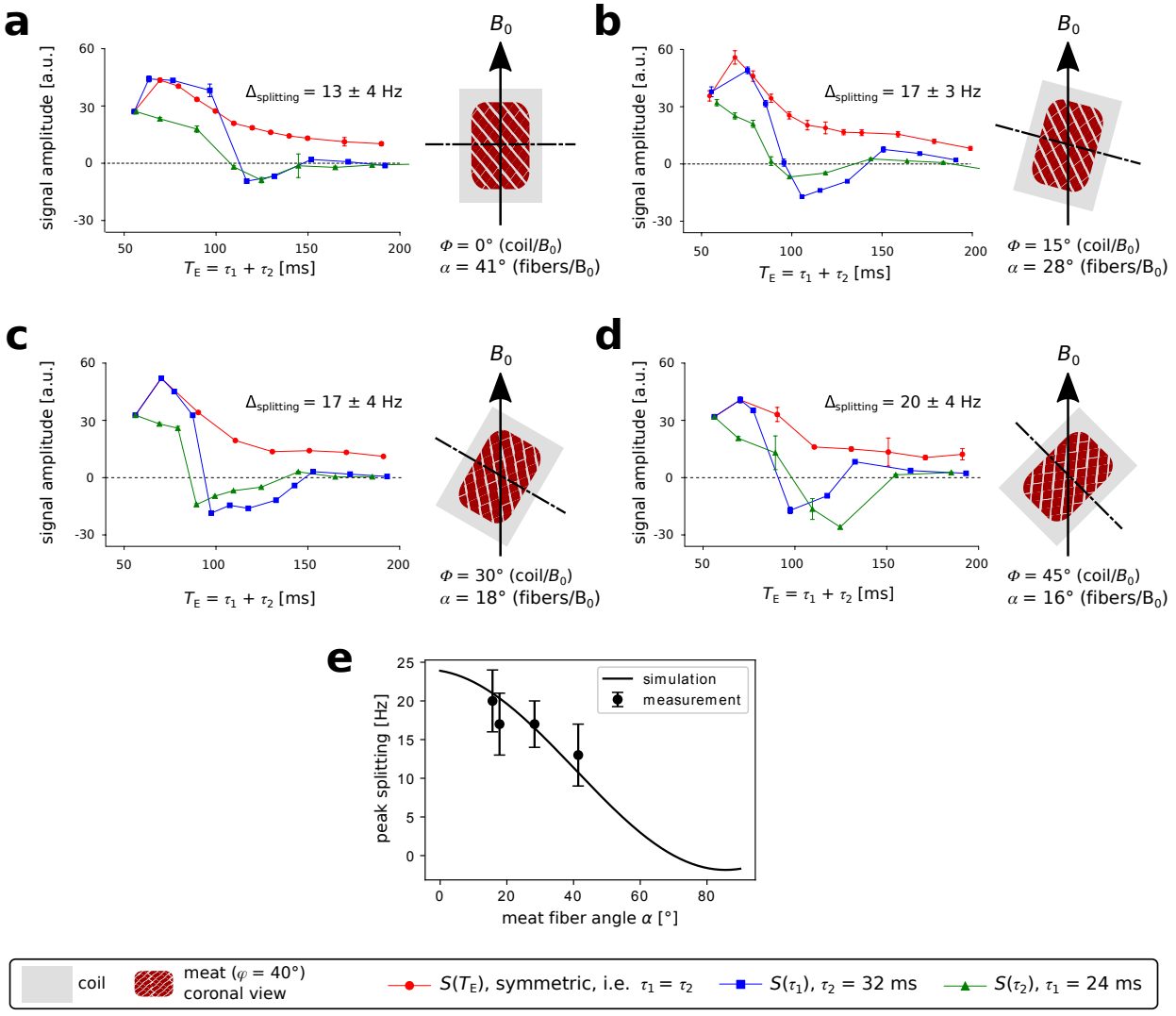

Figure 4: Signal sum of the fitted lactate doublet at 1.3 ppm as a function of the total echo time T_E with symmetric (red) and asymmetric (blue, green) composition of τ_1 and τ_2. The angle Φ of the coil (grey box) containing the meat specimen relative to the B_0 field was increased from 0° to 45° in the coronal plane (a-d). This decreased the effective muscle fiber angle α to B_0 (red hatching indicates the projection to the coronal plane, i.e. $\Phi - \varphi$) from 41° to 16° and leads to increased peak splitting of the lactate doublet (13 − 20 Hz). Peak splitting measured in spectra (e, black symbols) as a function of the measured muscle fiber orientation is in excellent agreement with simulations (black line) according to literature. Signal modulations of the lactate doublet for increasing echo times and different compositions of τ_1 and τ_2, are in good agreement with literature.

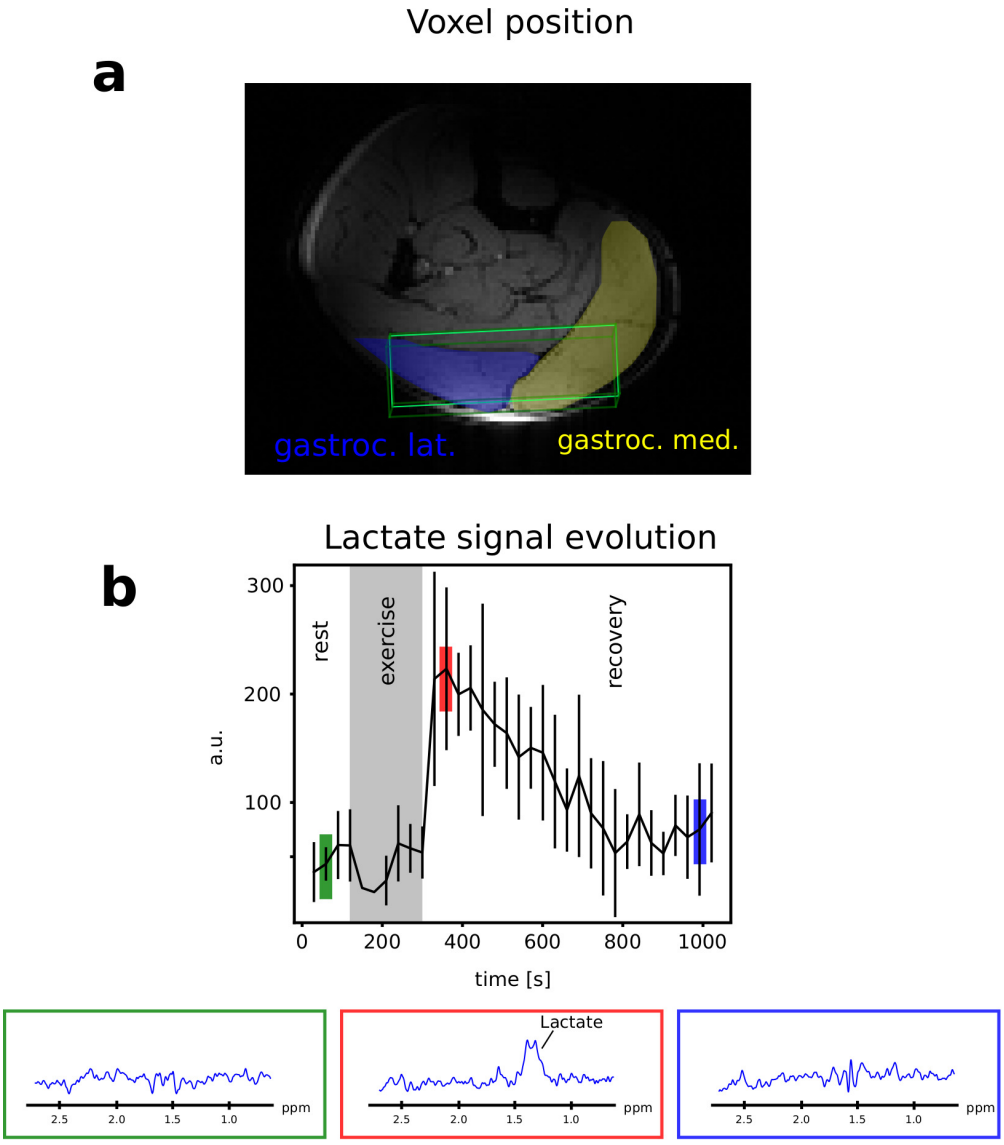

Figure 5: Transversal gradient-echo image of the calf from a representative subject with a typical voxel position for 3D localized semi-LASER and DQF-sLASER ^{1}H MRS covering m. gastrocnemius lateralis (blue) and m. gastrocnemius medialis (yellow) (a). Time course of fitted lactate concentrations (sum of fitted doublet areas averaged over all subjects, mean ± SD) during 2 min rest, 3 min plantar flexion exercise, free perfusion, and 12 min recovery (b). Ten consecutive spectra acquired in a representative subject were averaged (resulting in 30 s acquisition time per displayed spectrum), during rest (green), and early (red) / late (blue) recovery. Maximum lactate signal was observed approximately 1 min after the end of exercise visible as a clearly resolved doublet at 1.3 ppm.